

Supporting Information for *EES Batteries*

Zinc oxides reinforced silicon anodes for high-performance all-solid-state lithium-ion batteries

Renbo Liu^{a1}, Chaolin Mi^{a1}, Xiaobo Jiang^{a1}, Shijian Xiong^a, Zhengyang Song^a,
Yuanchang Shi^{a*}, Xiaohang Lin^{a*}, Peng Xiao^{b*}, Longwei Yin^a, Rutao Wang^{a,c,d*}

^a*Shandong Provincial Key Laboratory of Electrochemical Catalysis and Conversion, State Key Laboratory of Coatings for Advanced Equipment, School of Materials Science and Engineering, Shandong University, Jinan 250100, China.*

^b*State Grid Jiangsu Electric Power Co., Ltd. Research Institute, Nanjing 211103, China*

^c*Key Laboratory of Advanced Energy Materials Chemistry (Ministry of Education), Nankai University, Tianjin 300071, China.*

^d*Shandong Laboratory of Advanced Materials and Green Manufacturing at Yantai, Yantai 264003, China.*

¹These authors contributed equally to this work.

Email: Rtwang@sdu.edu.cn; yuanchangshi@sdu.edu.cn; lxh12345@sdu.edu.cn;
xiaop1@js.sgcc.com.cn

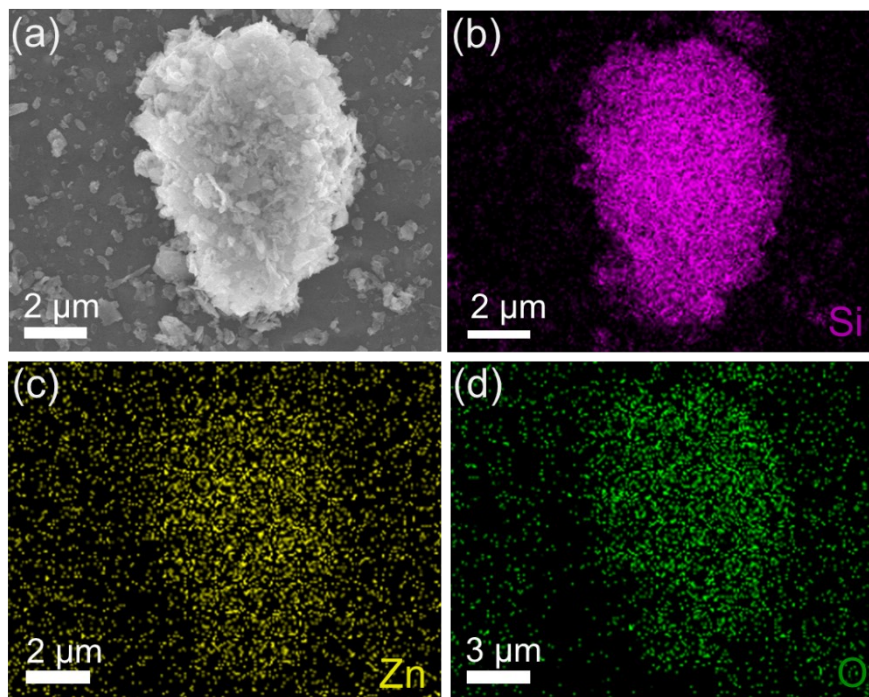


Figure S1. EDS mapping for Si-ZnO₄ sample from SEM.

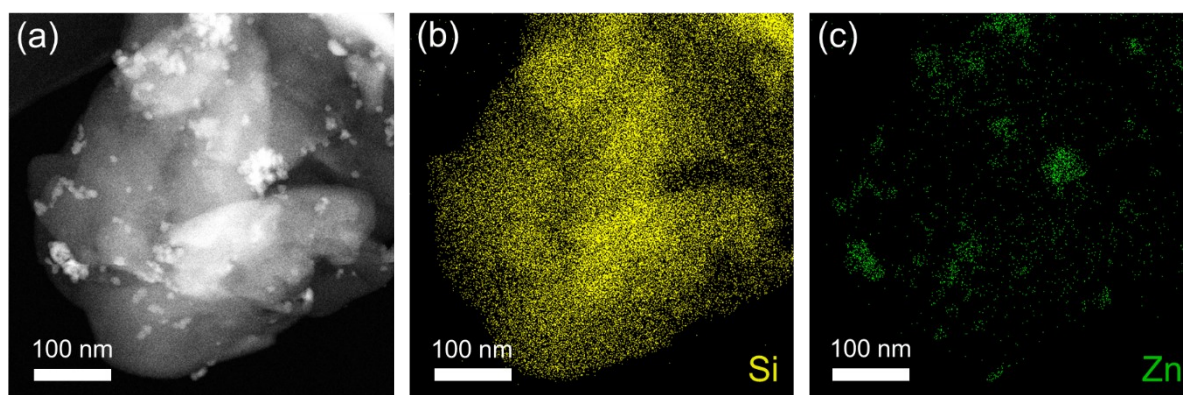


Figure S2. EDS mapping for Si-ZnO₄ sample from TEM.

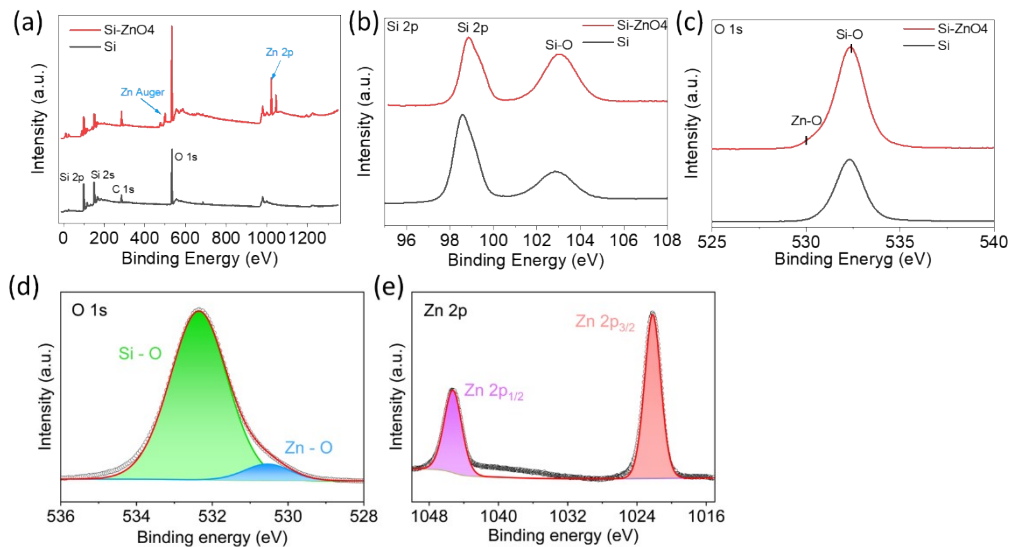


Figure S3. XPS spectra of Si-ZnO4 and Si anode. (a) Full-scale spectra, (b) Si 2p XPS spectra. (c) O 1s XPS spectra. (d) The deconvoluted O1s spectra for Si-ZnO4. (e) The deconvoluted Zn 2p spectra for Si-ZnO4.

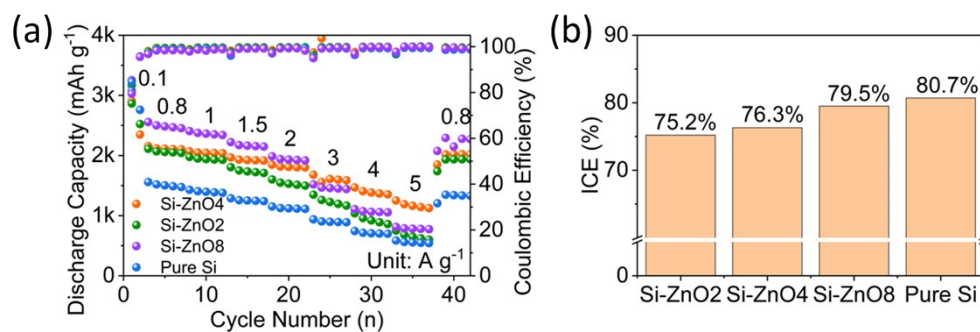


Figure S4. (a) Rate performance of Si-ZnO and pure Si samples. (b) Initial coulombic efficiency (ICE) values of Si-ZnO and pure Si samples.

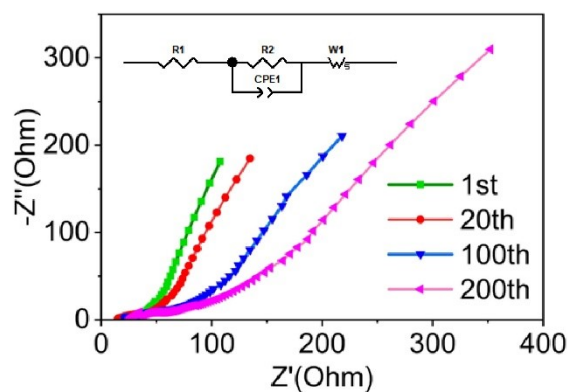


Figure S5. EIS spectra of Si-ZnO4 anode during the different cycling states.

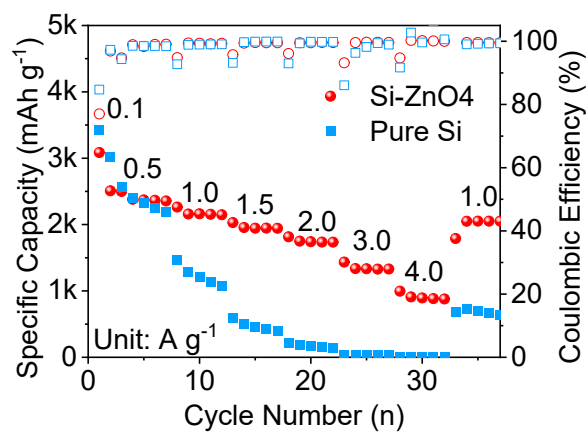


Figure S6. Rate performance of Si-ZnO and pure Si samples at room temperature.

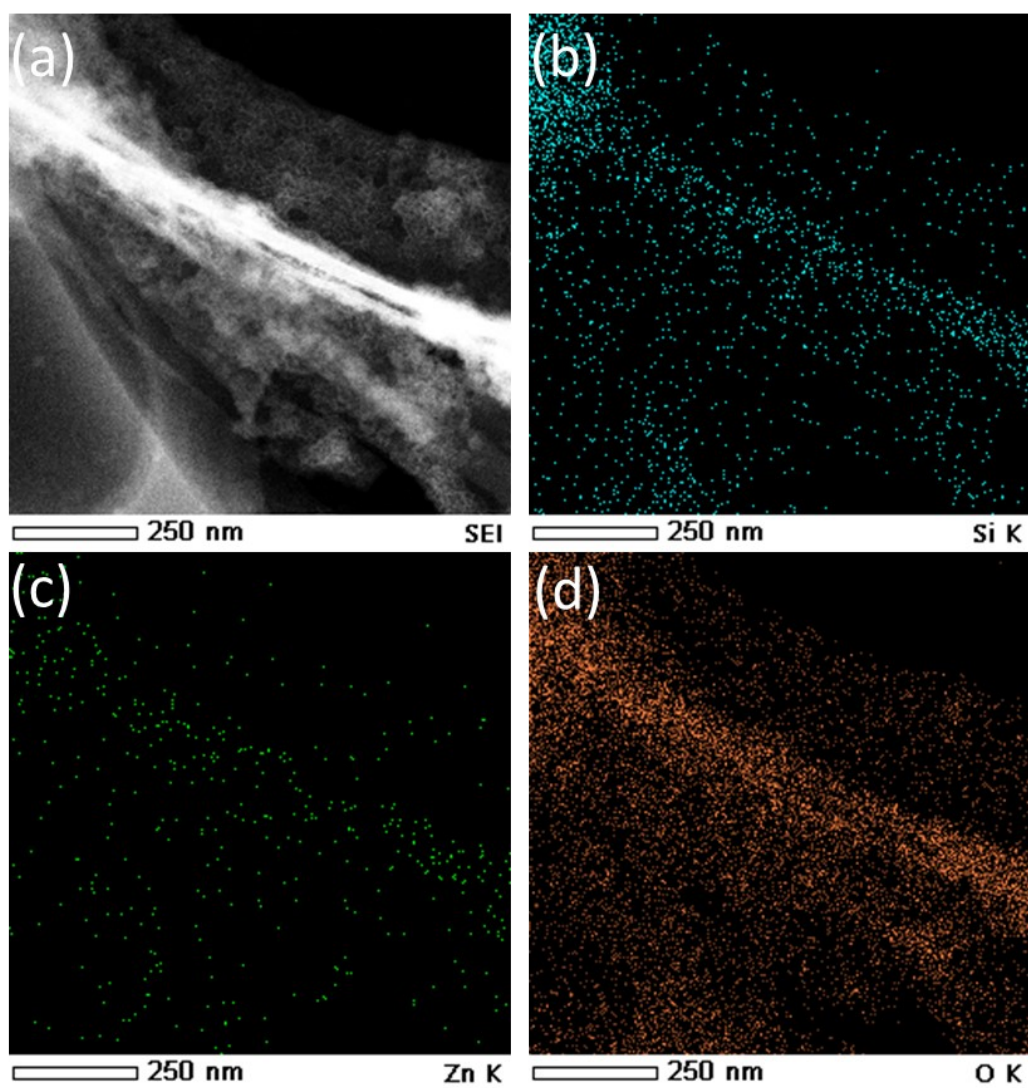


Figure S7. EDS mapping for Si-ZnO₄ anode from TEM at a delithiated state.

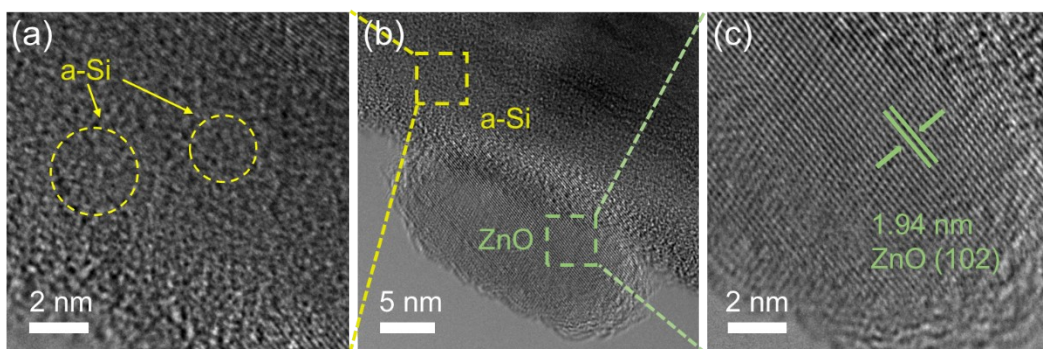


Figure S8. TEM images of Si-ZnO4 anode at a delithiated state and then exposed in air for 5 mins.

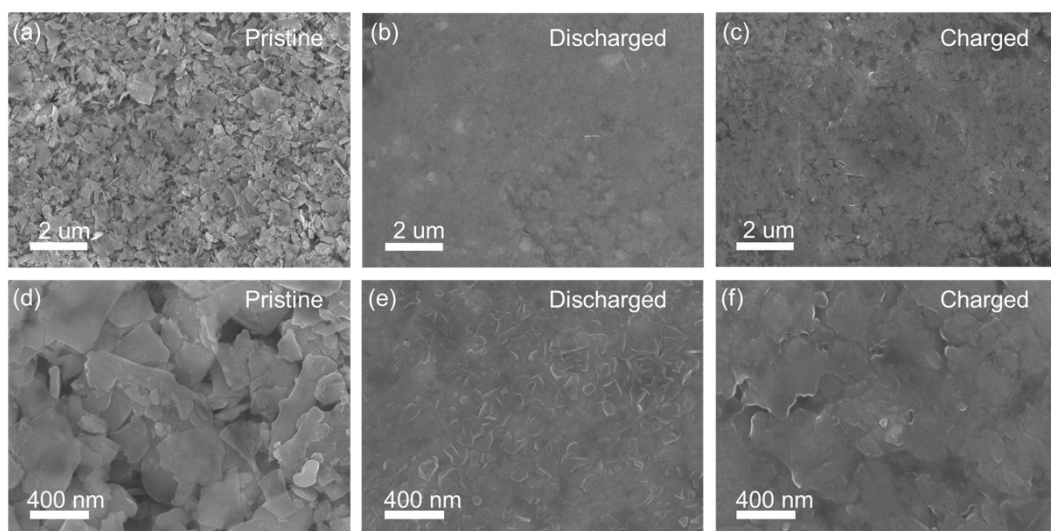


Figure S9. Top view of SEM images of Si-ZnO4 anode at (a) pristine state, (b) initial discharged state, and (c) initial charged state. (d-e) The corresponding magnified cross-section SEM images of Si-ZnO4 anode at these three states.

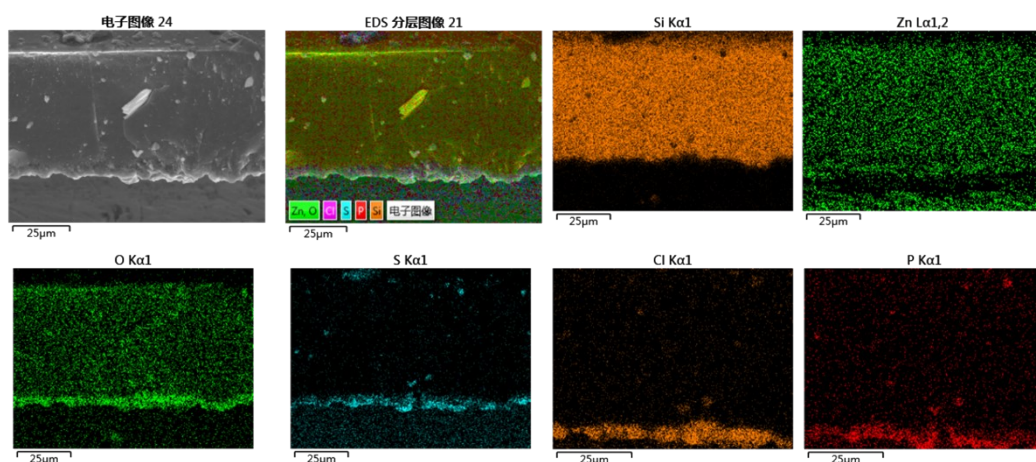


Figure S10. EDS mapping of Si-ZnO4 anode during the lithiated state.

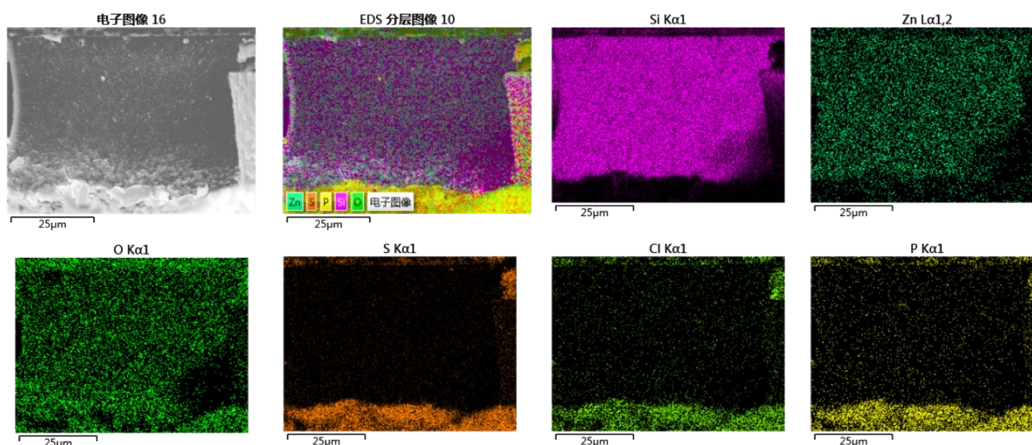


Figure S11. EDS mapping of Si-ZnO₄ anode during the delithiated state.

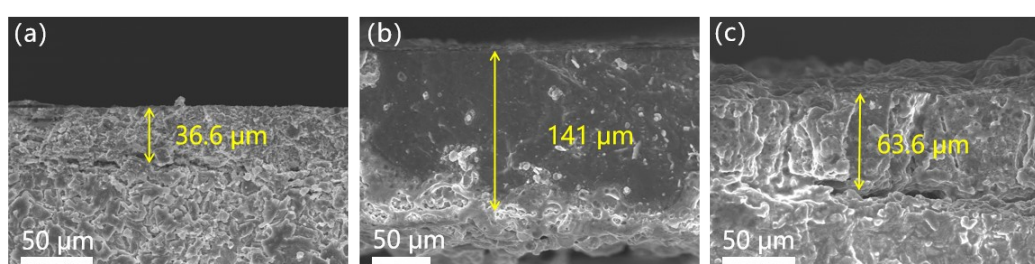


Figure S12. Cross-section SEM images of Si anode at (a) pristine state, (b) initial discharged state, and (c) initial charged state.

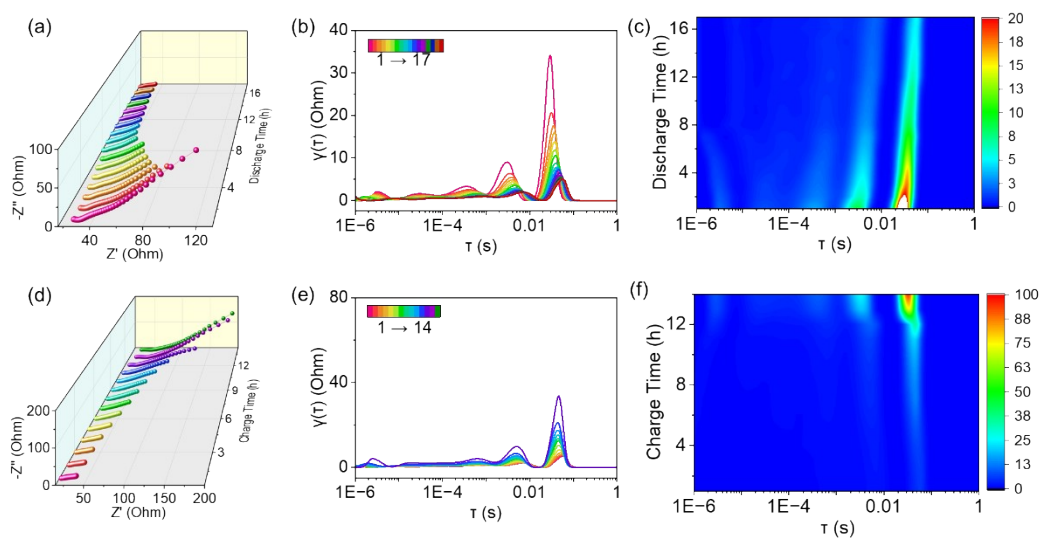


Figure S13. DRT analysis of Si anode. (a) EIS curves of Si anode in half-cell during discharging at 0.2 A g^{-1} and the corresponding DRT curves (b) and DRT contour map (c). (d) EIS curves of Si anode in half-cell during charging at 0.2 A g^{-1} and the corresponding DRT curves (e) and DRT contour map (f).

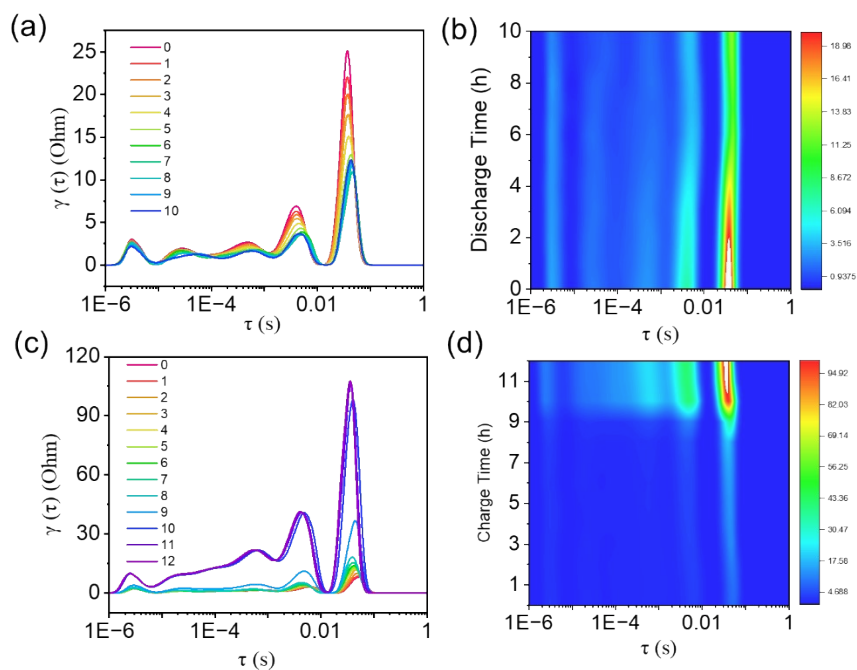


Figure S14. DRT analysis of Si-ZnO₄ anode after 20 cycles. (a) The DRT curves (a) and DRT contour map (b) of Si-ZnO₄ anode in half-cell during discharging at 0.2 A g⁻¹. (c) The DRT curves (c) and DRT contour map (d) of Si-ZnO₄ anode in half-cell during charging at 0.2 A g⁻¹.

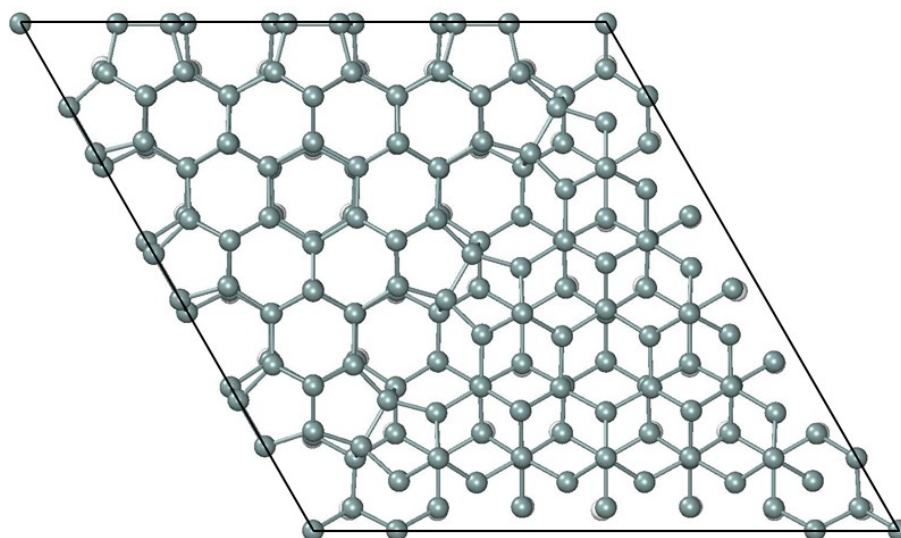


Figure S15. Si(111)-(7x7) reconstruction structure.

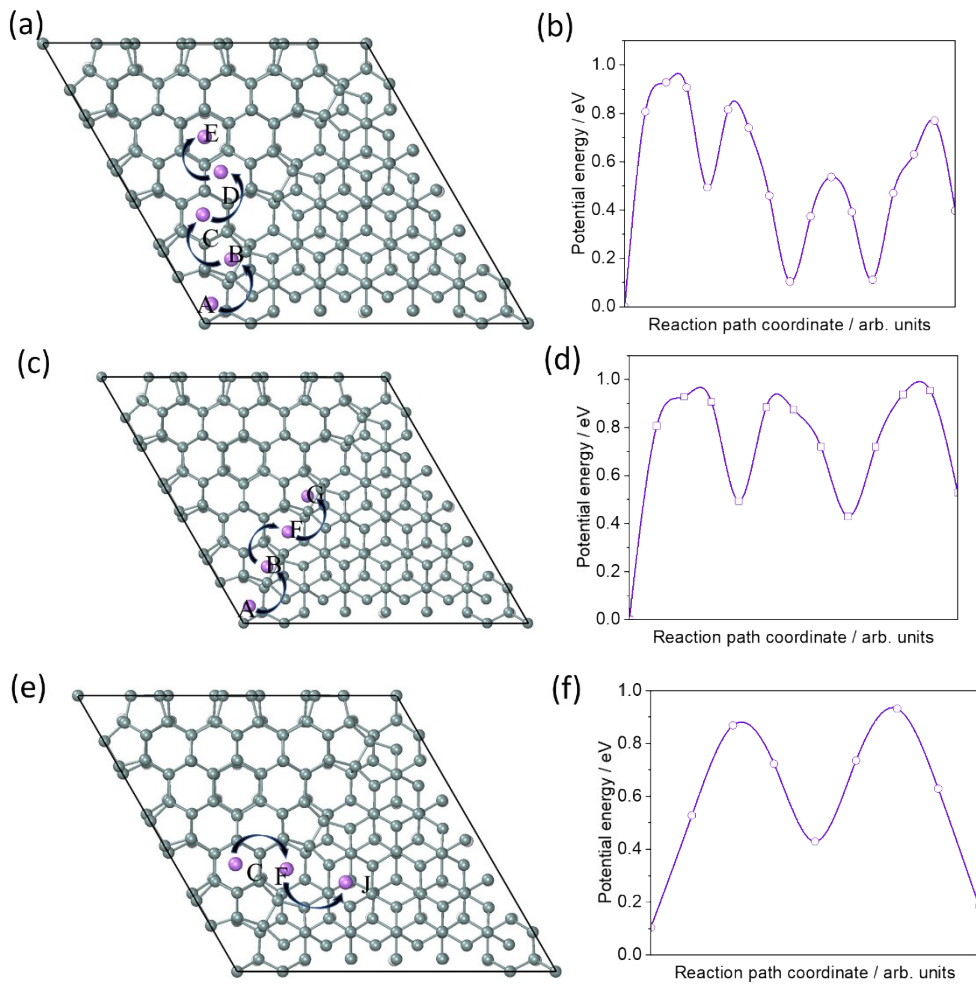


Figure S16. These diagrams showing other three possible Li⁺ diffusion paths on Si (111) ((a), (c), and (d)) and the corresponding migration energies ((b), (d), and (f)).